



# Semi-flowable Zn semi-solid electrodes as renewable energy carrier for refillable Zn–Air batteries

Daniel Perez-Antolin<sup>a,b,c</sup>, Wolfgang Schuhmann<sup>d</sup>, Jesus Palma<sup>a</sup>, Edgar Ventosa<sup>a,b,c,\*</sup>

<sup>a</sup> Electrochemical Processes Unit, IMDEA Energy, Avda. Ramón de la Sagra, 3, E-28935, Móstoles, Madrid, Spain

<sup>b</sup> Department of Chemistry, University of Burgos, Pza. Misael Bañuelos s/n, E-09001, Burgos, Spain

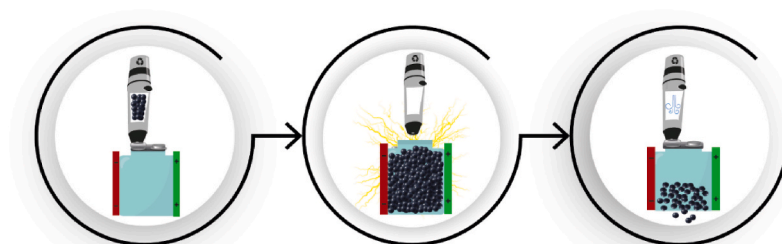
<sup>c</sup> International Research Centre in Critical Raw Materials-ICCRAM, University of Burgos, Plaza Misael Bañuelos s/n, E-09001, Burgos, Spain

<sup>d</sup> Analytical Chemistry – Center for Electrochemical Sciences (CES), Faculty of Chemistry and Biochemistry, Ruhr University Bochum, Universitätsstr. 150, D-44780, Bochum, Germany

## HIGHLIGHTS

- A new type of mechanically rechargeable Zn–Air batteries is demonstrated.
- Electrically conducting Zn slurries enable easy replacement of spent electrodes.
- Energy density of 1500 Wh L<sup>-1</sup> is achieved.
- Zn semi-solid electrodes become a new green energy carrier.
- Semi-solid electrodes present distinct advantages over gas and liquid fuels.

## GRAPHICAL ABSTRACT



## ABSTRACT

Today's society relies on energy storage on a day-to-day basis, e.g. match energy production and demand from renewable sources, power a variety of electronics, and enable emerging technologies. As a result, a vast range of energy storage technologies has emerged in the last decades. Among them, rechargeable Zn–Air batteries have held great promises for a long time. However, the severe challenges related to the reversible O<sub>2</sub> reactions and poor cyclability at the positive and negative electrodes, respectively, have severely hindered the success of this technology. Herein, electrically-conducting and semi-flowable Zn semi-solid electrodes are proposed to revive the appealing concept of a mechanically-rechargeable alkaline Zn–Air battery, in which the spent negative electrodes are easily substituted at the end of the discharge process (refillable primary battery). In this proof-of-concept study energy densities of ca. 1500 Wh L<sup>-1</sup> (1350 Ah L<sup>-1</sup><sub>electrode</sub> and utilization rate of 85%) are achieved thanks to the compromised flowability of the proposed Zn semi-solid electrodes. In this way, semi-solid Zn electrodes become a type of green energy carrier having intrinsic advantages over gas and liquid fuels. Zn semi-flowable electrode can be generated elsewhere using renewable sources, easily stored, transported, and used to produce electricity.

## 1. Introduction

Energy storage has become one of the main technological pillars of our society due to the increasing energy demand, the need for a sustainable energy model, and the emerging of off-grid power-demanding

gadgets. Obviously, the combination of a number of energy storage technologies will be required in the future to fulfill the various requirements of each specific application. Rechargeable batteries are the power sources of choice for portable electronics and they are called to power the upcoming generation of electric vehicles, most likely together

\* Corresponding author. Department of Chemistry, University of Burgos, Pza. Misael Bañuelos s/n, E-09001, Burgos, Spain  
E-mail address: [eventosa@ubu.es](mailto:eventosa@ubu.es) (E. Ventosa).

<https://doi.org/10.1016/j.jpowsour.2022.231480>

Received 23 February 2022; Received in revised form 28 March 2022; Accepted 14 April 2022

Available online 29 April 2022

0378-7753/© 2022 The Authors. Published by Elsevier B.V. This is an open access article under the CC BY-NC-ND license (<http://creativecommons.org/licenses/by-nc-nd/4.0/>).

with hydrogen fuel cells. Metal–Air batteries can be considered to be a nexus between the two named electrochemical technologies. As a result, metal–air batteries possess high specific energy (1084 Wh kg<sup>-1</sup> for Zn–Air) [1–3] because of the use of atmospheric air like in a fuel cell, while having a simple sealed architecture and a solid electroactive material, e.g. Zn or Li, like in a rechargeable battery. On the other hand, rechargeable metal–air batteries also have distinct disadvantages, i.e. lower energy efficiency related to the reversible O<sub>2</sub> reactions (both the OER and the ORR are using the same electrode) and poorer cycle stability associated with the reversible Zn reaction in a static configuration (sealed) cell [4,5]. In an attempt for overcoming the major challenges at once, the mechanically–rechargeable Zn–Air battery was proposed a long time ago, in which the spent negative electrodes are replaced at the end of the discharge process [6] [–] [13]. By doing this, two major issues are addressed: i) the poor cyclability of the Zn electrode in a static negative electrode, and ii) avoiding the oxygen evolution reaction in the air-breathing electrode during the charging process. In this way, spent Zn material can be collected and regenerated electrically in a separate cell specially designed for this process (e.g. electrowinning of Zn) or thermally in a concentrated solar power plant [2,11,14–17]. Two categories can be distinguished: i) substitution of the entire negative compartment, and ii) substitution of the spent negative electrode materials, also referred to as Zn/Air Fuel Cell (ZAFC) [7]. The latter approach has demonstrated to be suitable for practical implementation as several companies based their technology in this concept: the Electric Fuel Ltd., the Power Zinc, the Power Air Co., the Metallic Power Inc., and the Zinc8 [7,18–22]. In all cases, the poor electrical conductivity of ZnO locks achieving high volumetric capacities since large excess of electrolyte is used to promote the formation of dissolved zincates as discharge product and prevent ZnO formation. In this way, the volumetric capacity is largely locked by the solubility of zincates, which can be incrementally improved by using electrolyte additives or increasing the operating temperature [23]. However, the achieved volumetric capacities (100–150 Ah L<sup>-1</sup>) [24] are very far from the highly appealing value of Zn (5800 Ah L<sup>-1</sup>). Thus, innovative approaches are required to address this issue, which in turn will unlock the energy density of mechanically–rechargeable Zn–Air batteries.

In 2011, a pioneering work led by Chiang proposed for the first time the use of slurries in redox flow batteries [25]. These slurries contained solid redox-active particles, conducting additive and electrolyte forming flowable electrode, which were referred to as “semi-solid electrode”. Since then, the higher energy density of flowable semi-solid electrodes, compared to electrolytes containing dissolved species, have been exploited for different redox flow battery chemistries [26–28]. In addition, semi-solid electrodes offer other unique advantages such as enhanced mass transport due to their tunable porosity compared to conventional porous electrodes [29]. For instance, the company 24 M seizes the enhanced mass transport in semi-solid electrodes to manufacture Li-ion batteries having high areal capacities using non-flowable semi-solid electrodes [30]. So far, the two extreme cases have been used to develop innovative batteries, i.e. either highly flowable semi-solid electrodes or non-flowable semi-solid electrodes for redox flow and static batteries, respectively. Each case possesses pros and cons: flowable semi-solid electrodes results in lower energy density, while denser semi-solid electrodes that have higher energy density lacks the ability to flow. For instance, flowable Zn semi-solid electrodes have been deployed for Zn–Ni [31–33], and Zn–MnO<sub>2</sub> [34] redox flow batteries. The need for flowability resulted in Zn semi-solid electrodes of limited specific capacity. Specifically, values of 44.8 Ah L<sup>-1</sup> (52.4% utilization rate) [31], 40 Ah L<sup>-1</sup> (3% utilization rate) [32], 127.3 Ah L<sup>-1</sup> (58.44% utilization rate) [33], were achieved for redox flow Zn–Ni batteries. Note that static Zn pellets were used for the proof-of-concept of the semi-solid flow Zn–MnO<sub>2</sub> likely due to corrosion issues in neutral electrolyte. Recently, our group proposed the deployment of semi-solid electrodes of intermediate flowability to be used in static batteries. On the one hand, the resulting electrical percolation enables excellent

electrochemical performance and, on the other hand, they still present sufficient flowability to be injected and removed from the battery cell at the end-of-life to largely facilitate recyclability of static batteries [35]. This type of semi-flowable semi-solid electrodes are not feasible for redox flow batteries since the pumping consumption would be too high, but it enables eventual substitution.

In this context, our goal is to revive the promising concept of mechanically–rechargeable Zn–Air batteries that implies the use of Zn as energy carrier. To regain attention, high practical energy densities need to be achieved. With this aim, we propose for the first time the use of electrically-conducting and semi-flowable semi-solid electrodes in non-flow Zn–Air batteries (refillable primary battery). Previous studies on Zn semi-solid electrodes achieved relatively low energy density due to constrictions derived from the need for continuous flow and for its electrochemical recharging process in the same device. Our concept of using Zn semi-solid electrode in non-flow mechanically rechargeable Zn–Air batteries widens the range of carbon content since semi-flowable viscous slurries are valid for our case. The semi-solid and semi-flowable nature of our electrodes provides not only the proposed Zn-based electrodes with sufficient flowability to recharge mechanically a Zn/Air battery, but also the electrical percolating network and deformability to minimize passivation of remaining active material by formation of ZnO. By this, the volumetric capacity in semi-flowable Zn electrodes is boosted opening up a new research direction for reaching the full potential of mechanically–rechargeable Zn–Air batteries. Alkaline Zn-based semi-solid electrodes are suggested to act as green energy carriers since Zn metal can be electrochemically generated (Zn electrowinning) from discharge products. This concept may become of high interest for a number of emerging applications in which neither batteries nor fuel cells completely fulfill the requirements.

## 2. Materials and methods

### 2.1. Reagents and materials

Zinc powder (99.9% –100 mesh, Alfa Aesar), Carbon additive KetjenBlack EC-600 JD (Azelis and AkzoNovel polymer chemicals), KOH (≥85%, Sigma Aldrich), were used as-received. Expanded graphite (Sigracet TF6) was used as negative current collector, Celgard 3501 as separator and E4B (ElectricFuel) as air electrode. Gaskets were made of Viton® due to its resistance to alkaline conditions.

### 2.2. Preparation and formulation of semi-solid electrodes

Semi-solid electrodes with different compositions were prepared using 6, 20, 26, 42 wt% active material, corresponding with 0.1, 0.33, 0.5 and 1 kg<sub>Zn</sub> L<sub>electrode</sub><sup>-1</sup>. In addition, 4.5, 2.9, 3.7 and 1.4 wt% of carbon additive, respectively, was used. Active material proportion was calculated by dividing the amount of active material (grams of Zn or carbon additive) by the total weight of the solid materials (carbon additive and zinc).

$$\text{wt. \%}_A = \frac{g_A}{g_{\text{Solid}}} \cdot 100$$

The solid particles were dispersed in 6 mL of electrolyte (6 M KOH) and mixed with Ultra-Turrax IKA T18-Basic during three periods of 10 min resting 5 min between period. The slurries were prepared directly in a syringe to facilitate the injection of the electrode into the battery pre-assembled.

### 2.3. Materials and fabrication of refillable cells

The external casing of the battery was designed and printed by FDM-3D-Printing machine (MakerBot Replicator™ 2X) using Acrylonitrile butadiene styrene (ABS) for planar configuration and by Selective Deposition Lamination-3D-Printing machine (Anycubic: Photon Mono

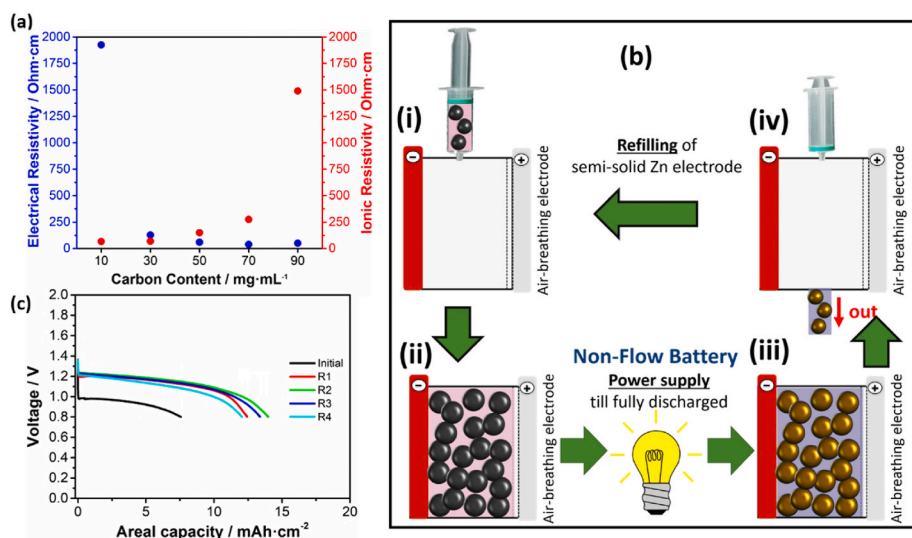


**Fig. 1.** (a) Electrical and ionic resistivities of semi-solid electrodes containing different carbon contents (10, 30, 50, 70, 90 mg<sub>C</sub>·mL<sup>-1</sup>) (b) Schematic representation of the working principle of the mechanically-rechargeable semi-solid Zn-Air battery. (i) A pre-assembled electrochemical cell is filled with flowable semi-solid Zn electrode. (ii) The cell is sealed and ready to deliver energy in static (non-flow) configuration. (iii) The sealed cell reaches full state of discharge. (iv) The spent semi-solid Zn electrode is removed from the cell, which is then ready to be refilled in step (i). (c) Voltage profile of 5 subsequent refilling using a semi-solid electrode containing 0.1 kg<sub>Zn</sub> L<sup>-1</sup> electrode in 6 M KOH.

SE) using Grey Colored UV resin (Anycubic) for the tubular one.

#### 2.4. Electrochemical characterization

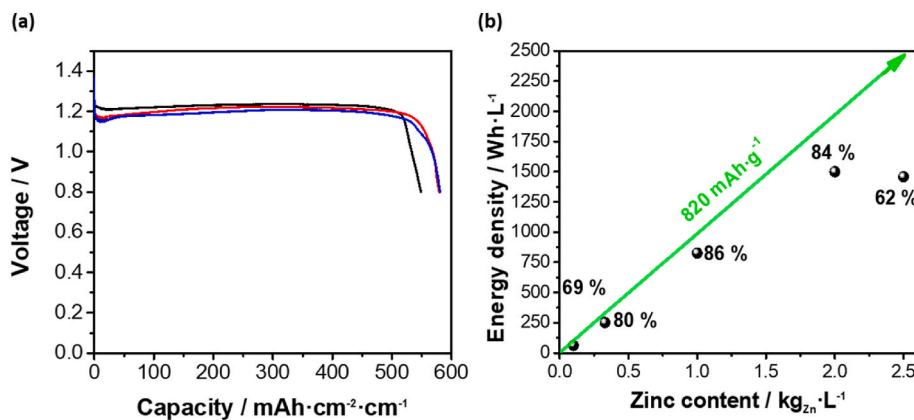
Electrochemical testing of the battery was carried out using a battery tester (Neware BTS4000 5V6A).

### 3. Results and discussion

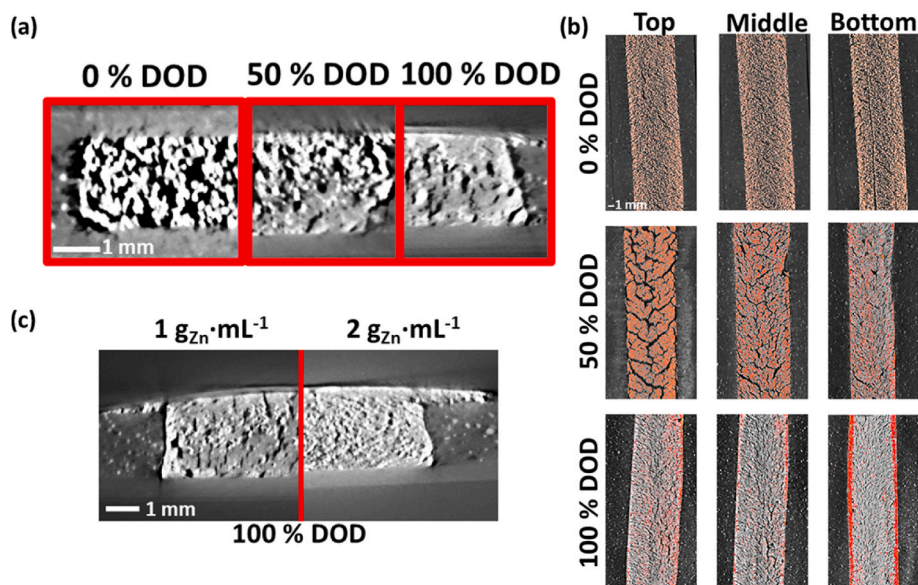
#### 3.1. Proof-of-concept of mechanically rechargeable Zn-air battery based on Zn semi-solid electrodes

Fig. 1a shows the evolution of the ionic and electrical resistivity of an electrolyte containing suspended carbon particles as a function of the carbon content (Section S1, Fig. S1, S2). Whereas the ionic resistivity increased with increasing carbon content due to the hindrance of the solid particles as in conventional porous battery electrodes, electrical resistivity decreased with increasing carbon content. This reveals that electrochemically active and flowable semi-solid electrodes can be obtained through tuning of composition formulation. In our case, the value of 70 mg mL<sup>-1</sup> represents a balanced tradeoff between electrical and ionic resistivity, so that carbon contents around this value were explored in further formulations containing Zn particles (below). Implementation of the new vision for a mechanically-rechargeable Zn-Air battery chemistry requires the design and fabrication of a reusable primary

battery cell. This consists of an air-breathing electrode capable of reducing oxygen from the atmosphere and a compartment capable of allocating Zn-based semi-solid electrode, as positive and negative electrode, respectively. These electrodes are electrically separated by a microporous separator (Section S2, Fig. S3). In a way, this easily refillable primary battery becomes a fuel cell, in which the typically employed gas or liquid fuel (e.g. H<sub>2</sub>, methanol) is replaced by a semi-solid fuel. As a result, cheap microporous separator can be used instead of an ion-selective membrane. Fig. 1b illustrates the working principle in a sequence of 4 steps. The key technology enabler in our work is the use of electrically percolated and flowable Zn semi-solid electrodes (dense suspension of Zn and carbon additive in an alkaline electrolyte). The use of these semi-solid electrodes allows for the realization of the sequence of steps shown in Fig. 1b. Fig. 1c shows the voltage profiles of 5 subsequent refilling cycles using the same cell but substituting the Zn semi-solid electrode according to the refilling procedure illustrated in Fig. 1b. After a first slightly poorer-performing discharge, the operating voltage and areal capacity remained stable. A value of 13 mAh cm<sup>-2</sup> with a high Zn utilization rate in the range of 67–77% (546–633 mAh g<sub>Zn</sub><sup>-1</sup>) for R1–R4 were achieved at ca. 0.1C (16 mA cm<sup>-2</sup>). It should be noted that the reproducibility is limited by the oversimplified refilling method was applied in this work. This method is based on the removal of spent semi-solid electrode using a stream of tap water (Section S3, Fig. S4) and the refilling of fresh semi-solid electrode using a simple syringe (manually injected, Fig. S5). Although the



**Fig. 2.** (a) Voltage profiles of three subsequent injections. (b) Energy density evolution for semi-solid electrodes with different zinc content (0.1 kg<sub>Zn</sub> L<sup>-1</sup>, 0.33 kg<sub>Zn</sub> L<sup>-1</sup>, 1 kg<sub>Zn</sub> L<sup>-1</sup>, 2 kg<sub>Zn</sub> L<sup>-1</sup> and 2.5 kg<sub>Zn</sub> L<sup>-1</sup>).



**Fig. 3.** X-ray computed tomography (a) Cross section of semi-solid electrodes at different Depth-Of-Discharge (0%, 50% and 100%). (b) Top-view of electrodes at different semi-solid heights (top, bottom and middle) with different DOD. (c) Cross section of two electrodes with different Zn content ( $1 \text{ kg}_{\text{Zn}} \cdot \text{L}^{-1}$  and  $2 \text{ kg}_{\text{Zn}} \cdot \text{L}^{-1}$ ) at 100% DOD.

method enabled substitution of semi-solid electrodes for this proof-of-concept, much effort is required from an engineering perspective to improve the reproducibility and overall performance of the system.

### 3.2. Tuning of energy density by changing the Zn content in the semi-solid electrode

The independent content of Zn and carbon additive enables tuning of energy density and specific power, separately. The energy density of a semi-solid electrode is determined by the content of Zn. That is, the higher content ( $\text{kg}_{\text{Zn}} \cdot \text{L}_{\text{electrode}}^{-1}$ ), the higher volumetric charge capacity ( $\text{Ah} \cdot \text{L}^{-1}$ ), and thus higher energy density ( $\text{Wh} \cdot \text{L}^{-1}$ ). Fig. 2a shows typical voltage profiles, which were used to calculate the energy density as integral under the curves. Note that volume is calculated as area by thickness of the cavity in which the semi-solid electrode is injected:  $7 \text{ cm}^2 \times 0.2 \text{ cm}$ . Fig. 2b shows the evolution of the energy density achieved (voltage profiles in Section S4, Fig. S6) as a function of the content of Zn ( $\text{kg}_{\text{Zn}} \cdot \text{L}_{\text{electrode}}^{-1}$ ).

The increase in energy density was almost perfectly linear with increasing Zn content, being close to the theoretical values represented as a green arrow in Fig. 2b. At higher value of Zn content ( $2 \text{ kg}_{\text{Zn}} \cdot \text{L}^{-1}$ ), higher material utilization of 84% ( $687 \text{ mAh} \cdot \text{g}_{\text{Zn}}$ ) was achieved at  $32 \text{ mA} \cdot \text{cm}^{-2}$  (ca. 0.1C). This resulted in a value of energy density of  $1500 \text{ Wh} \cdot \text{L}^{-1}$ , that is calculated considering the volume of carbon, Zn and electrolyte. Values of energy density at cell level (including separator, current collector and air-breathing electrode) are discussed below. Note that the value of energy density only decreases 5% at cell level including separator, current collector and air-breathing electrode. It should also be noted that a remarkable areal capacity of  $303 \text{ mAh} \cdot \text{cm}^{-2}$  was here demonstrated at 0.1C ( $32 \text{ mA} \cdot \text{cm}^{-2}$ ), which is relevant for the energy density of the entire device. These values not only largely exceed typical values reported for conventional Zn-Air batteries, but also recent reports using solid-state electrolyte. That is, the value achieved in our work ( $303 \text{ mAh} \cdot \text{cm}^{-2}$  at  $32 \text{ mA} \cdot \text{cm}^{-2}$ ) is 3-fold higher than the state-of-the-art value of  $133 \text{ mAh} \cdot \text{cm}^{-2}$  at the current density of  $4 \text{ mA} \cdot \text{cm}^{-2}$ , which is in turn 100 times higher than that of the Zinc-Air battery using zinc foil as anode ( $1\text{--}2 \text{ mAh} \cdot \text{cm}^{-2}$ ) [36].

### 3.3. Exploring the limits of energy density by X-ray tomography

For Zn content above  $2 \text{ kg} \cdot \text{L}^{-1}$ , the utilization rate of Zn significantly decreased, i.e. 62 % at  $2.5 \text{ kg}_{\text{Zn}} \cdot \text{L}^{-1}$ . This is likely due to clogging issue related to the formation of ZnO as discharge product. X-ray computed tomography analysis (Fig. 3) was carried out to investigate the microstructures of Zn semi-solid electrodes and the changes upon discharge process.

To facilitate the visualization, the evolution of microstructure of the semi-solid electrode with the depth-of-discharge (DOD) was first studied for intermediate Zn content ( $1 \text{ kg}_{\text{Zn}} \cdot \text{L}^{-1}$ ). Fig. 3a shows the cross-section images of a Zn semi-solid electrode ( $1 \text{ kg}_{\text{Zn}} \cdot \text{L}^{-1}$ ) at various DOD (0%, 50% and 100%). And Fig. 3b shows top-views of these 3 samples at 3 different electrode depth (top: near Air-breathing electrode, middle: between current collector and air-breathing electrode, and bottom: near current collector). At 0% DOD (fully charged), a homogenous distribution of Zn particles, which are visualized as bright areas in Fig. 3a and orange spots in Fig. 3b, was observed. At 100% DOD, Zn particles were almost completely oxidized leading to the disappearance of the bright areas (orange spots in Fig. 3b). The most interesting image corresponds to 50% DOD. Two regions are distinguished in this image: top is brighter (intense orange in Fig. 3b) and bottom is darker (lighter orange in Fig. 3b). This indicates that Zn particles were preferentially oxidized at the bottom. The air breathing electrode was located at the top while negative current collect was located at the bottom. This means that the ionic transport ( $\text{OH}^-$  anions) from the air-breathing electrode to the current collector across the semi-solid electrode is sufficient so that the reaction takes place preferentially close to the current collector. This special feature of semi-solid electrodes is due to the higher porosity and enhanced mass transport of semi-solid electrodes, compared to conventional electrodes, and enable progressive transformation from the current collector towards the air-breathing electrode. This is highly beneficial since the opposite behavior (formation of ZnO near the air-breathing electrode) that is observed for thick conventional electrodes leads to blockage of ionic pathways from the air-breathing electrode to the rest of the electrode [37]. The preferential formation of ZnO starting from the current collector towards the air-breathing electrode avoid this blockage for anion transport to active Zn particles, which results in deep discharge and high utilization of Zn. Fig. 3c shows the cross-section images of semi-solid electrode at 100% DOD (fully discharged) for 2

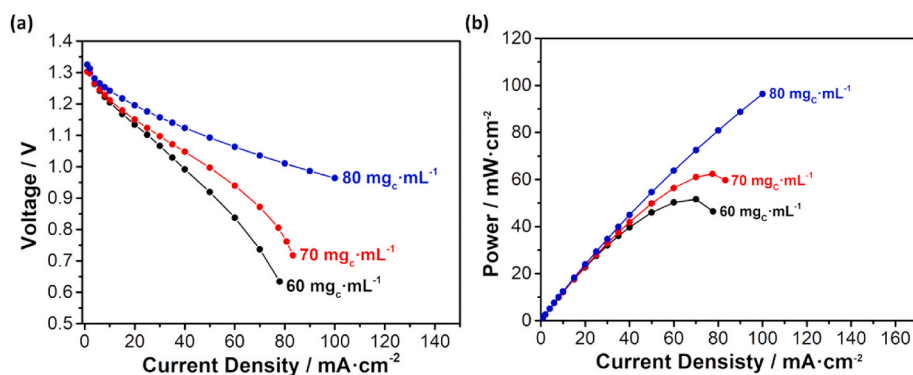


Fig. 4. Performance of semi-solid electrodes with different formulation in terms of (a) evolution of the operating voltage and (b) evolution of the specific power with the applied current density for a Zn content of 0.5 kg L<sup>-1</sup>.

different Zn contents, i.e. 1 kg<sub>Zn</sub> L<sup>-1</sup> and 2 kg<sub>Zn</sub> L<sup>-1</sup>. While micro-channels were still visible for 1 kg<sub>Zn</sub> L<sup>-1</sup>, the spent electrode for 2 kg<sub>Zn</sub> L<sup>-1</sup> is completely dense. Consequently, maintaining high utilization rates (e.g. >80%) becomes difficult for this electrode composition when Zn contents are higher than 2 g<sub>Zn</sub> mL<sup>-1</sup>, as shown in Fig. 2a. Reformulation and re-optimization of the semi-solid electrode is therefore necessary to achieve high utilization rates for higher Zn content.

### 3.4. Tuning specific power by changing the content of carbon in semi-solid electrodes

The specific power and voltage efficiency of the proposed concept will largely depend on the overall resistance of the semi-solid electrodes. Fig. 4a and b displays the evolution of the operating voltage and the corresponding evolution of specific power, respectively, as a function of the applied current density for various formulations (electrochemical data and voltage efficiencies in Section S5, Fig. S7). Due to the balanced tradeoff between electrical and ionic conductivity shown for the semi-solid electrode containing 70 mg mL<sup>-1</sup>, the content of Zn was fixed at 0.5 g mL<sup>-1</sup> and the carbon content was varied around 70 mg mL<sup>-1</sup>, i.e. 60, 70 and 80 mg mL<sup>-1</sup>, to illustrate the influence of carbon content in the specific power. For comparison, the specific power measurements were carried out at 50% depth of discharge (DOD). Fig. S8 (Section S6) shows the evolution of the internal resistance with the DOD revealing stable resistance from 0% to 90. Thus, different behavior for the specific power is anticipated when the cells are almost discharge (>90% DOD).

In general, the specific power increases with increasing carbon content, while flowability decreases. Electrodes containing 80 mg<sub>carbon</sub>mL<sup>-1</sup> were able to deliver ca. 100 mW cm<sup>-2</sup> at 100 mA cm<sup>-2</sup> (1 V). However, we were unable to remove this semi-solid electrode by applying our simple removal protocol (tap water), while electrodes containing lower carbon contents (60–70 mg<sub>carbon</sub>mL<sup>-1</sup>) were easily removed. In general, this home-made device using a low-cost MnO<sub>x</sub>-

based air-breathing electrode and semi-flowable semi-solid Zn electrodes (60–70 mg<sub>carbon</sub>mL<sup>-1</sup>) is demonstrated to operate at current densities in the range of 50 mA cm<sup>-2</sup>. At this current density, a specific power value of >50 mW cm<sup>-2</sup> was delivered without a critical loss in voltage efficiency (>80%), which are remarkable values considering the thickness of the electrode (>100 mAh cm<sup>-2</sup>). Since the three main elements of the cell, i.e. Mn-based air-breathing electrode, microporous separator, and stainless-steel current collector (Section S7, Fig. S9) are inexpensive, power costs (USD kW<sup>-1</sup>) rapidly decay in the range of 1–5 mA cm<sup>-2</sup> (Section S7, Fig. S10). Thus, the values of current density demonstrated in this work result in a cost of power below 100 USD kW<sup>-1</sup>, approaching the asymptote in the curve of power cost vs. current density.

### 3.5. Boosting the specific power by implementing redox mediators

Incremental improvements in the specific power can be achieved by optimizing the formulation of the semi-solid electrode. However, the use of conventional conductive particles for providing electrical conductivity requires physical contact between carbon particles for reaching electrical percolation. The presence of high contents of carbon both hinders ionic conductivity and reduces flowability, so that innovative strategies are of high interest. In this context, we explored the use of a molecular wire to support electrical conductivity. When a reversible redox species is dissolved in the electrolyte and its redox potential is above that of the oxidation of Zn metal, spontaneous charge transfer reaction can take place between dissolved species and Zn metal. As a result, Zn metal is oxidized and dissolved species are reduced. The reduced dissolved species can then diffuse to the carbon network, where they are oxidized being able to react again with Zn metal (Fig. 5a). The 2,6-dihydroxyanthraquinone (2,6-DHAQ) has been used in alkaline aqueous redox flow batteries [38], showing a redox potential of ca. -0.7 V vs SHE, which is above the redox potential of Zn/ZnO(- 1.25 V vs

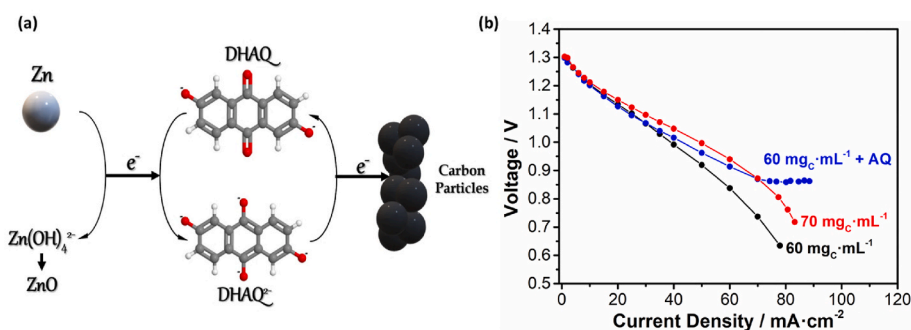
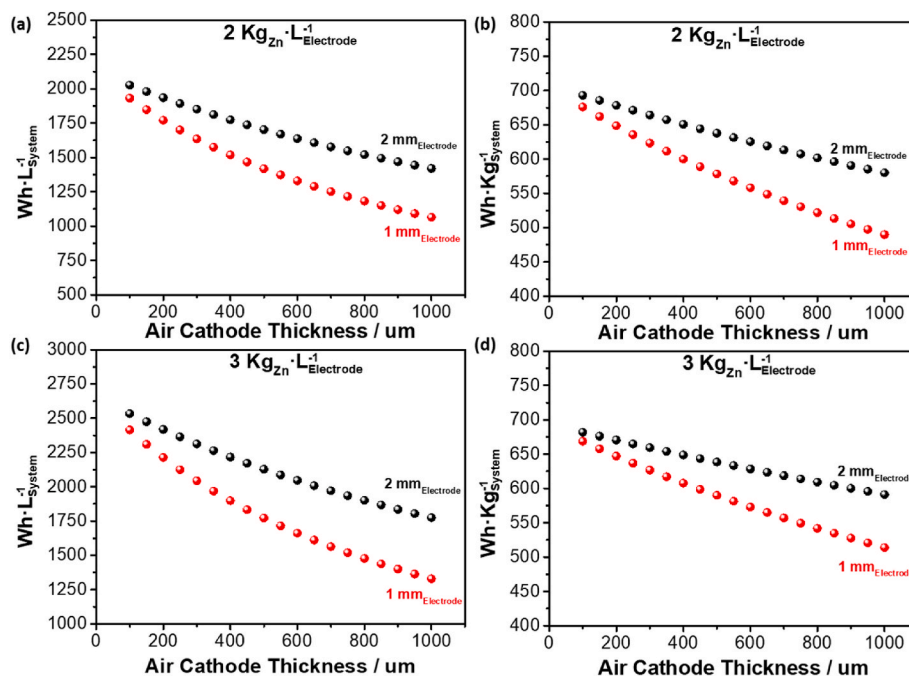


Fig. 5. (a) Scheme of 2,6-dihydroxyanthraquinone acting as molecular wiring for mechanically rechargeable semi-solid Zinc-Air battery. (b) Comparison of the operating voltage when 2,6-dihydroxyanthraquinone is included into the formulation of the electrode.



**Fig. 6.** Theoretical estimation of energy density for Zn-Air batteries using semi-solid electrodes. Comparison between two different Zinc content in the electrode: (a) and (b) for  $2 \text{ kg}_{\text{Zn}} \text{ L}^{-1}$ , and (c) and (d) for  $3 \text{ kg}_{\text{Zn}} \text{ L}^{-1}$ . Thickness of Celgard separator and stainless-steel current collector are 0.025 mm and 0.012 mm, respectively.

SHE). Thus, charge transfer reaction between 2,6-DHAQ and Zn should thermodynamically occur since  $E_{\text{reduction}} > E_{\text{oxidation}}$  ( $\Delta G < 0$ ). Indeed, 2,6-DHAQ has been recently used as molecular wire for metal hydrides in redox flow batteries [39]. Considering the redox potentials, dissolved 2,6-DHAQ should be able to be reduced to 2,6-DHAQ<sup>2-</sup> while Zn metal oxidizes to ZnO. If so, the reduced anthraquinone can transport these charges by diffusing across the porous electrode to the current collector, where the applied potential drives its oxidation back to its neutral state transferring the charges originated from the Zn metal. In other words, 2,6-DHAQ can act as a molecular wire (Fig. 5a). Fig. 5b shows the evolution of cell voltage as a function of the applied current density for semi-solid electrode containing  $60 \text{ mg mL}^{-1}$ ,  $70 \text{ mg mL}^{-1}$  and  $60 \text{ mg mL}^{-1}$  in the presence of dissolved 2,6-DHAQ ( $0.5 \text{ kg}_{\text{Zn}} \text{ L}^{-1}$  for all of them).

Considering that the open cell voltage (Zn-Air) was ca. 1.45 V and the difference between the redox potential of Zn/ZnO and 2,6-DHAQ/2,6-DHAQ<sup>2-</sup> is ca. 0.55 V, the reduced 2,6-DHAQ (after spontaneous reaction with Zn) should be re-oxidized at the current collector when the operating cell voltage is 0.9 V. In Fig. 5b, for the same amount of carbon ( $60 \text{ mg mL}^{-1}$ ), the performance for the semi-solid in the presence of 2,6-DHAQ starts to improve at ca. 0.95 V, which confirms the function of the molecular wire for this semi-solid electrode. Indeed, the presence of 2,6-DHAQ was able to outperform an excess of carbon in the semi-solid electrode, i.e.  $60 \text{ mg mL}^{-1}$  with mediators versus  $70 \text{ mg mL}^{-1}$  without mediator. Above the value of  $70 \text{ mA cm}^{-2}$  (0.88 V), the specific power of the semi-solid electrode containing 2,6-DHAQ was remarkable, compared to semi-solid electrodes containing even more amount of carbon. It should be noted that we were not able to apply current density above  $90 \text{ mA cm}^{-2}$  due to limitation of the instrument when operating below 1 V. Therefore, the use of molecular wire not only enables the use of less amount of carbon, which is very beneficial for the flowability, but it actually increases the specific power compared with semi-solid electrodes containing higher amounts of carbon. It should be noted that self-discharge does not occur when the semi-solid electrode is stored outside the cell before injection. In addition, there is much room for improvement in terms of specific power by combining engineering and colloidal chemistry in future studies.

### 3.6. Projected specific energy and energy density of mechanically rechargeable Zn-Air batteries based on semi-solid electrodes

Engineering aspects obviously play an important role for the practical energy density of the proposed technology. We conducted a theoretical analysis to assess the potential of the concept. The influence of two critical parameters, i.e. thickness of air-breathing electrode and thickness of the semi-solid electrode, on the energy density and specific energy was analyzed for two Zn contents,  $2 \text{ kg}_{\text{Zn}} \text{ L}^{-1}$  (demonstrated in this work) and  $3 \text{ kg}_{\text{Zn}} \text{ L}^{-1}$  (target for future works). The contribution of casing that is rather large in our home-made prototypes is not considered to elucidate the intrinsic values. We consider that the contribution of casing should be addressed at a later stage (after reaching higher Technology Readiness Level), while intrinsic values provide a better idea of the potential of this technology. Fig. 6 reveal three important points. I) The use of a thick electrodes, as in our work, is beneficial for all studied cases. This is due to that fact that the volume losses of inactive elements, e.g. current collector and separator, are minimized with increasing areal capacity. II) The energy density increases as the thickness of the air-breathing electrode decreases. This is due to that fact that  $\text{O}_2$  is in the air so that the volume of the air-breathing electrode does not limits the charge storage capacity of the cell. And III) the benefit of using thick semi-solid electrodes is reduced with decreasing thickness of the air-breathing electrode. This is due to the volume of inactive elements decreases with decreasing thickness of air-breathing electrode, so that the positive impact of thick semi-solid electrode is buffered. This latter point may be of interest for higher power applications that requires thinner semi-solid electrodes.

In this work, the thickness of the air-breathing electrode and the Zn content in the semi-solid electrodes were  $0.5 \text{ mm}$  and  $2 \text{ kg L}^{-1}$ , respectively. This results in values of ca.  $1703 \text{ Wh L}^{-1}$  and  $638 \text{ Wh kg}^{-1}$  when 100% utilization rates are achieved. If the utilization rate is reduced to 84% (demonstrated here), the energy density only decreases to  $1430 \text{ Wh L}^{-1}$ . It should be noted that energy density only decreases 5% with respect to the energy density of the electrode ( $1500 \text{ Wh L}^{-1}$ ) when including separator, current collector and air-breathing electrode are also considered. For a Zn content of  $3 \text{ kg L}^{-1}$  and a utilization rate of 80%, the energy density would be  $1700 \text{ Wh L}^{-1}$ , which indicates both Zn

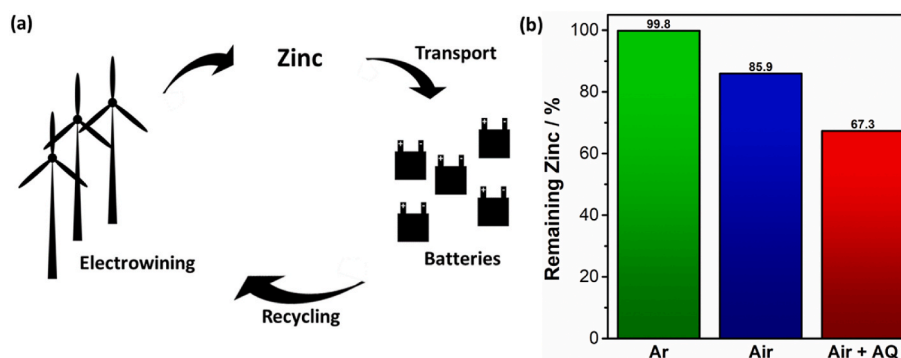


**Fig. 7.** (a) Scheme of metallic zinc as energy carrier used in mechanically-rechargeable Zn–Air batteries. (b) Self-discharge of Zn: results of experiments for determining the amount of zinc that remains when it is stored in different conditions: Ar-filled, Air-filled and Air-filled in the presence of 2,6-DHAQ in the electrolyte.

content and utilization rate are relevant to achieve high values of energy density.

### 3.7. Zn semi-solid electrodes as potential energy vector

The mechanically-rechargeable Zn–Air battery can be considered as a refillable primary Zn – Air battery that uses Zn as renewable energy carrier (Fig. 7a). The spent ZnO can be easily dissolved in e.g. mild acid media and transported in liquid phase to the regeneration site. By the mature and well-established Zn electrowinning process [40,41],  $Zn^{2+}$  ions are reduced to metal Zn using energy from renewable sources. Zn semi-solid electrode can be prepared and stored in sealed containers for their transportation. Refilling of the device can be conducted directly from these containers. The most critical point here is the self-discharge during storage/transportation. Due to the strong alkaline media used in this work, spontaneous reaction of Zn and water is kinetically slow. To evaluate the self-discharge rate, Zn particles were stored in 6 M KOH for 24 h and, then, the loss of Zn was determined.

Due to the higher solubility of zincates at increasing KOH concentration, Zn particles were rinsed with 12 M KOH after storage, dried it and weighted it. When the suspension of Zn was stored under protected atmosphere (Ar-filled), the loss of Zn was negligible (0.2 wt%) (Fig. 7b). However, when the suspension of Zn was purged with air, a loss of 14.1 wt% was observed after 24 h. When the suspension of Zn contained redox wire (anthraquinone), the kinetics between oxygen reduction and Zn oxidation increased, and the loss of Zn increased up to 32.7 wt%. Considering that low-cost microporous are often used in Zn–Air batteries, slow diffusion of oxygen from the air-breathing electrode to the negative electrode cannot be avoided. It should be noted that self-discharge that occurs by diffusion of oxygen or the charged molecular wire is prevented by storing the semi-solid electrode in containers before its use. Importantly, exclusion of air from the containers storing Zn semi-solid electrodes should be considered for storage and transport.

## 4. Conclusions

In summary, success of the concept of a mechanically-rechargeable Zn–Air battery has been locked by the poor practical energy density of semi-flowable Zn electrodes ( $\approx 150 \text{ Wh L}^{-1}$ ) due to the formation of passivating ZnO. This concept has been long desired since it overcomes the most demanding challenges of Zn–Air batteries (reversible oxygen reaction and Zn reaction) by decoupling the charge and discharge process of a Zn–Air battery in the two processes in separate device. However, the low practical energy densities have been so far achieved in practice. In our work, the use of electrically conducting flowable semi-solid electrodes unlocks the achievement of higher practical volumetric capacities (ca.  $1500 \text{ Wh L}^{-1}$ ) using a 3-D printed home-made primary Zn–Air battery cell. The cells were mechanically recharged several times, thus demonstrating successfully the feasibility of the

concept. These values were achieved by comprising flowability of the semi-solid electrodes, while their semi-flowability still enables eventual substitution of electrode (in contrast to continuous flow for redox flow batteries). This opens up a new research direction in the field of energy storage, in which Zn-based semi-solid electrodes become a new type of renewable fuel. In contrast to gas and liquid fuel, Zn semi-flowable “fuel” is easier to be stored, transported, used in an electrochemical cell due to its semi-solid nature (active material is solid and easier to be confined). This battery concept has the potential to become a fitting power source for a number of emerging and demanding applications such as drones, in which safety, fast charge and high energy density are essential. Nevertheless, intensive efforts are required to be devoted from neighboring fields such as colloidal chemistry, chemical engineering and mechanical engineering to make this concept more competitive.

## Notes

The authors declare no competing financial interest.

## CRediT authorship contribution statement

**Daniel Perez-Antolin:** Methodology, Investigation, Visualization, Writing – original draft. **Wolfgang Schuhmann:** Investigation, Resources. **Jesus Palma:** Supervision, Funding acquisition. **Edgar Ventosa:** Conceptualization, Methodology, Writing – review & editing, Supervision, Funding acquisition.

## Declaration of competing interest

The authors declare that they have no known competing financial interests or personal relationships that could have appeared to influence the work reported in this paper.

## Acknowledgment

The project leading to these results has received funding from “la Caixa” Foundation, under agreement LCF/PR/PR18/51130007” and the Spanish Government through the Research Challenges Programme (Grant RTI2018-099228-A-I00). E.V. thanks the MINECO for the financial support (RYC2018-026086-I).

## Appendix A. Supplementary data

Supplementary data to this article can be found online at <https://doi.org/10.1016/j.jpowsour.2022.231480>.

## References

- [1] J.-S. Lee, S. Tai Kim, R. Cao, N.-S. Choi, M. Liu, K.T. Lee, J. Cho, Metal-air batteries with high energy density: Li-air versus Zn-air, *Adv. Energy Mater.* 1 (2011) 34–50, <https://doi.org/10.1002/aenm.201000010>.
- [2] Y. Li, H. Dai, Recent advances in Zinc-air batteries, *Chem. Soc. Rev.* 43 (2014) 5257–5275, <https://doi.org/10.1039/c4cs00015c>.
- [3] A.R. Mainar, E. Iruin, L.C. Colmenares, A. Kvasha, I. de Meaza, M. Bengoechea, O. Leonet, I. Boyano, Z. Zhang, J.A. Blazquez, An overview of progress in electrolytes for secondary zinc-air batteries and other storage systems based on zinc, *J. Energy Storage* 15 (2018) 304–328, <https://doi.org/10.1016/j.est.2017.12.004>.
- [4] Q. Liu, Z. Pan, E. Wang, L. An, G. Sun, Aqueous metal-air batteries: fundamentals and applications, *Energy Storage Mater.* 27 (2020) 478–505, <https://doi.org/10.1016/j.ensm.2019.12.011>.
- [5] S. Hosseini, S. Masoudi Soltani, Y.Y. Li, Current status and technical challenges of electrolytes in zinc-air batteries: an in-depth review, *Chem. Eng. J.* 408 (2021), 127241, <https://doi.org/10.1016/j.cej.2020.127241>.
- [6] T.C. Group, P.C. Foller, Improved slurry zinc/air systems as batteries for urban vehicle propulsion, *J. Appl. Electrochem.* 16 (1986) 527–543, <https://doi.org/10.1007/BF01006848>.
- [7] P. Sapkota, H. Kim, Zinc-air fuel cell, a potential candidate for alternative energy, *J. Ind. Eng. Chem.* 15 (2009) 445–450, <https://doi.org/10.1016/j.jiec.2009.01.002>.
- [8] J.W. Evans, G. Savaskan, M. Engineering, A zinc-air cell employing a packed bed anode, *J. Appl. Electrochem.* 21 (1991) 105–110, <https://doi.org/10.1007/BF01464289>.
- [9] M.J. Korall, Y. Harats, J. Sassen, J.R. Goldstein, US5418080A, 1994.
- [10] J.F. Cooper, D. Fleming, L. Keene, A. Maimoni, K. Peterman, R. Koopman, Demonstration of Zinc/air Fuel Battery to Enhance the Range and Mission of Fleet Electric Vehicles: Preliminary Results in the Refueling of a Multicell Module, *Intersoc. Energy Convers. Eng. Conf. CA (United States)*, 1994, pp. 7–12. <https://ui.adsabs.harvard.edu/abs/1994iece.conf....7C/abstract>. (Accessed 4 February 2021).
- [11] J. Goldstein, I. Brown, B. Koretz, New developments in the electric fuel zinc-air system, in: *Int. Power Sources Symp.*, 1999, pp. 171–179, [https://doi.org/10.1016/S0378-7753\(98\)00260-2](https://doi.org/10.1016/S0378-7753(98)00260-2), 80 (1–2).
- [12] J.R. Goldstein, B. Koretz, *Intersoc. Energy Convers. Eng. Conf.* 28 (1993), 2.279.
- [13] M.S. and J.F.C. J. Noring, S. Gordon, A. Maimoni, Mechanically refuelable zinc/air electric vehicle cells, *Electromechanical Soc. Meet. Honolulu, HI.* (1993) 16–21.
- [14] D. Selvakumaran, A. Pan, S. Liang, G. Cao, A review on recent developments and challenges of cathode materials for rechargeable aqueous Zn-ion batteries, *J. Mater. Chem. A.* 7 (2019) 18209–18236, <https://doi.org/10.1039/c9ta05053a>.
- [15] F. Wang, O. Borodin, T. Gao, X. Fan, W. Sun, F. Han, A. Faraone, J.A. Dura, K. Xu, C. Wang, Highly reversible zinc metal anode for aqueous batteries, *Nat. Mater.* 17 (2018) 543–549, <https://doi.org/10.1038/s41563-018-0063-z>.
- [16] M.I. Petrescu, G. V Ghica, T. Buzatu, Recovery of zinc and manganese from spent batteries by reductive leaching in acidic media, *J. Power Sources* 247 (2014) 612–617, <https://doi.org/10.1016/j.jpowsour.2013.09.001>.
- [17] I.G. and M.G. J. R. Goldstein, N. Lapidot, M. Aguf, Electric Fuel Zinc-Air System: Zinc Regeneration Update, *Electrochem. Soc. Pennington, NJ.* (1997) 97(18), 881.
- [18] Electric Fuel, (n.d.). <https://electric-fuel.com/>. (Accessed 8 June 2021).
- [19] Powerzinc, (n.d.). <http://www.powerzinc.com/>. (Accessed 8 June 2021).
- [20] Metallic Power, (n.d.). <http://www.metallicpower.com/>. (Accessed 8 June 2021).
- [21] S. Smedley, Zinc air fuel cell for industrial and specialty vehicles, *IEEE Aero. Electron. Syst. Mag.* 15 (2000) 19–21, <https://doi.org/10.1109/62.891975>.
- [22] The Leader in Zinc Air Battery Technology - Zinc8 Energy Solutions, (n.d.). <https://www.zinc8energy.com/>(accessed June 8, 2021).
- [23] B. Koretz, J.R. Goldstein, I. Gektin, Electric Fuel™ zinc-air battery regeneration technology presented, in: *Annu. Meet. Appl. Electrochem. Div. Ger., Chem. Soc.*, 1995.
- [24] N.J. Cherepy, R. Krueger, J.F. Cooper, A Zinc/Air Fuel Cell for Electric Vehicles, *Annu. Batter. Conf. Long Beach, CA*, 1999.
- [25] M. Duduta, B. Ho, V.C. Wood, P. Limthongkul, V.E. Brunini, W.C. Carter, Y. M. Chiang, Semi-solid lithium rechargeable flow battery, *Adv. Energy Mater.* 1 (2011) 511–516, <https://doi.org/10.1002/aenm.201100152>.
- [26] E. Ventosa, D. Buchholz, S. Klink, C. Flox, L.G. Chagas, C. Vaalma, W. Schuhmann, S. Passerini, J.R. Morante, Non-aqueous semi-solid flow battery based on Na-ion chemistry. P2-type Na<sub>x</sub>Ni<sub>0.22</sub>Co<sub>0.11</sub>Mn<sub>0.66</sub>O<sub>2</sub>-NaTi<sub>2</sub>(PO<sub>4</sub>)<sub>3</sub>, *Chem. Commun.* 51 (2015) 7298–7301, <https://doi.org/10.1039/c4cc09597a>.
- [27] Z. Li, K.C. Smith, Y. Dong, N. Baram, F. Fan, J. Xie, Aqueous Semi-solid Flow Cell: Demonstration and Analysis, 2013, pp. 2–7.
- [28] F.Y. Fan, W.H. Woodford, Z. Li, N. Baram, K.C. Smith, A. Helal, G.H. Mckinley, W. Craig Carter, M. Chiang, Polysulfide flow batteries enabled by percolating nanoscale conductor networks, *Nano Lett.* 14 (2014), <https://doi.org/10.1021/nl500740t>.
- [29] D. Muñoz-Torrero, J. Palma, R. Marcilla, E. Ventosa, Al-ion battery based on semisolid electrodes for higher specific energy and lower cost, *ACS Appl. Energy Mater.* 3 (2020) 2285–2289, <https://doi.org/10.1021/acsaem.9b02253>.
- [30] 24M Technologies, (n.d.). <https://24-m.com/>(accessed April 20, 2020).
- [31] J. Liu, Y. Wang, Preliminary study of high energy density Zn/Ni flow batteries, *J. Power Sources* 294 (2015) 574–579, <https://doi.org/10.1016/j.jpowsour.2015.06.110>.
- [32] Y.G. Zhu, T.M. Narayanan, M. Tulodziecki, H. Sanchez-Casalogue, Q.C. Horn, L. Meda, Y. Yu, J. Sun, T. Regier, G.H. McKinley, Y. Shao-Horn, High-energy and high-power Zn–Ni flow batteries with semi-solid electrodes, *Sustain. Energy Fuels* 4 (2020) 4076–4085, <https://doi.org/10.1039/D0SE00675K>.
- [33] Y. Liu, Q. Hu, J. Zhong, Z. Wang, H. Guo, G. Yan, X. Li, W. Peng, J. Wang, A renewable sedimentary slurry battery: preliminary study in zinc electrodes, *iScience* 23 (2020), <https://doi.org/10.1016/j.isci.2020.101821>.
- [34] T.M. Narayanan, Y.G. Zhu, E. Gençer, G. McKinley, Y. Shao-Horn, Low-cost manganese dioxide semi-solid electrode for flow batteries, *Joule* 5 (2021) 2934–2954, <https://doi.org/10.1016/j.joule.2021.07.010>.
- [35] D. Perez-Antolin, R. Trócoli, J. Palma, E. Ventosa, The injectable battery. A conceptually new strategy in pursuit of a sustainable and circular battery model, *J. Power Sources* 480 (2020), 228839, <https://doi.org/10.1016/j.jpowsour.2020.228839>.
- [36] Y. Zuo, K. Wang, S. Zhao, M. Wei, X. Liu, P. Zhang, Y. Xiao, J. Xiong, A high areal capacity solid-state zinc-air battery via interface optimization of electrode and electrolyte, *Chem. Eng. J.* 430 (2022), 132996, <https://doi.org/10.1016/j.cej.2021.132996>.
- [37] C.Y. Jung, T.H. Kim, W.J. Kim, S.C. Yi, Computational analysis of the zinc utilization in the primary zinc-air batteries, *Energy* 102 (2016) 694–704, <https://doi.org/10.1016/j.energy.2016.02.084>.
- [38] K. Lin, Q. Chen, M.R. Gerhardt, L. Tong, S.B. Kim, L. Eisenach, A.W. Valle, D. Hardee, R.G. Gordon, M.J. Aziz, M.P. Marshak, Alkaline quinone flow battery, *Science* 349 (2015) 1529–1532, [https://doi.org/10.1126/SCIENCE.AAB3033/SUPPL\\_FILE/LIN.SM.PDF](https://doi.org/10.1126/SCIENCE.AAB3033/SUPPL_FILE/LIN.SM.PDF) (80-).
- [39] T. Páez, F.F. Zhang, M.Á. Muñoz, L. Lubian, S. Xi, R. Sanz, Q. Wang, J. Palma, E. Ventosa, The redox-mediated nickel–metal hydride flow battery, *Adv. Energy Mater.* (2021), 2102866, <https://doi.org/10.1002/AENM.202102866>.
- [40] J. St-Pierre, D.L. Piron, Electrowinning of zinc from alkaline solutions, *J. Appl. Electrochem.* 16 (1986) 447–456.
- [41] A.E. Saba, A.E. Elsherief, Continuous electrowinning of zinc, *Hydrometallurgy* 54 (2000) 91–106, [https://doi.org/10.1016/S0304-386X\(99\)00061-4](https://doi.org/10.1016/S0304-386X(99)00061-4).